

Electromotive Force of the High-Temperature Concentration Cell Using Al-Doped CaZrO₃ as the Electrolyte

Jinxiao Bao¹, Hiroyuki Ohno^{1,*}, Yuji Okuyama², Norihiko Fukatsu¹ and Noriaki Kurita¹

¹Department of Materials Science and Engineering, Graduate School of Engineering, Nagoya Institute of Technology, Nagoya 466-8555, Japan

²Environmental Technology Research Division, INAMORI Frontier Research Center, Kyushu University, Fukuoka 819-0395, Japan

In order to clarify the electrochemical properties of the Al-doped CaZrO₃ system, a gas concentration cell was assembled adopting 0.4 mol% Al-doped CaZrO₃ polycrystalline sintered material as the electrolyte and its electromotive force (emf) was measured for various oxygen and hydrogen chemical potential gradients. The measurements were performed in a hydrogen-rich atmosphere for the temperature range from 973 to 1473 K. For almost all the conditions in the experiment, the measured emf's were well explained by regarding that the substantial predominant charge carrier is the proton. Under the conditions that the transport number of proton is less than unity, the agreement was examined between the measured emf and the theoretical one estimated based on the conduction parameters determined by the conductivity measurement reported in the previous work. It was confirmed that they well coincide with each other in all experimental conditions.

This fact shows that the conduction parameters of CaZr_{0.996}Al_{0.004}O_{3-α} and also the model of defect structure reported in the previous work were reasonable. The proton conduction domain of Al-doped CaZrO₃ in the oxygen-hydrogen chemical potentials plane was examined based on these conduction parameters and it was found to be a little wider than that of In-doped CaZrO₃ system. [doi:10.2320/matertrans.M2012020]

(Received January 10, 2012; Accepted January 31, 2012; Published March 14, 2012)

Keywords: hydrogen sensor, calcium zirconate, proton conductor, solid electrolyte, conduction domain diagram

1. Introduction

As a solid electrolyte has the properties of both solid and ion conductor, it has been generally utilized conveniently for chemical sensors, fuel cells, coulometric measurement devices, etc. Especially, proton-conducting solid electrolyte CaZr_{0.9}In_{0.1}O_{3-α} is chemically and mechanically stable at high temperatures. Therefore, it has been applied for molten metal hydrogen sensors and further practical applications are ongoing.¹⁻⁵⁾ Meanwhile, in some temperature and surrounding atmosphere conditions, positive hole or oxygen ion conduction would occur in addition to the proton conduction; in that case the output of the sensor would be affected not only by the hydrogen concentration but also by the oxygen concentration. In order to broaden such applications, it is necessary to grasp its electrochemical properties exactly in regard to temperature and surrounding atmosphere conditions.⁶⁻⁹⁾

In recent years, we have been studying the electrochemical properties of CaZrO₃-based oxides under high temperatures and a wide range of hydrogen and oxygen potentials. For Al-doped CaZrO₃, we recently reported the result of conductivity measurement and proposed conduction parameters for this system.¹⁰⁾ In the present report, the emf of the gas concentration cell utilizing the polycrystalline CaZr_{0.996}Al_{0.004}O_{3-α} as the electrolyte was investigated in order to confirm the validity of the conduction parameters and understand the electrochemical properties of the system in more detail.

2. Experimental

2.1 Theoretical formula of cell

Here, we consider the emf of the following gas concentration cell theoretically.

(ref., -), Pt', mixed gas ($\mu'_{\text{O}_2}, \mu'_{\text{H}_2}$) | CaZr_{0.996}Al_{0.004}O_{3-α} | mixed gas ($\mu''_{\text{O}_2}, \mu''_{\text{H}_2}$), Pt'', (+, meas.)

When an electrolyte is kept in a state where the activities of the charge carrier-relating component are kept at different values at their ends, an electrical potential difference occurs across the electrolyte. Wagner derived the emf generated across the electrolyte under the condition that the component gradient and the electronic conduction are included. The electrical potential gradient established in the electrolyte is given as follows.¹¹⁾

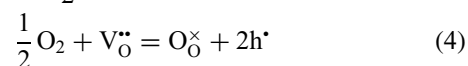
$$\frac{d\phi}{dx} = -\frac{1}{F} \sum_i (t_i/z_i) d\mu_i/dx \quad (1)$$

where ϕ is the potential of internal electrolyte, and F is the Faraday constant, t_i is the transport number of charge carrier i , z_i is the valence of the charge carrier and μ_i is the chemical potential of the charge carrier.

If we assume that the charge carriers are interstitial protons, H_i^+ , positive holes, h^+ , oxide ion vacancies, $\text{V}_\text{O}^{\bullet\bullet}$, and excess electrons, e' , the formula becomes as follows.

$$d\phi = -\frac{1}{F} \left(t_{\text{H}_i^+} d\mu_{\text{H}_i^+} + t_{\text{h}^+} d\mu_{\text{h}^+} + \frac{1}{2} t_{\text{V}_\text{O}^{\bullet\bullet}} d\mu_{\text{V}_\text{O}^{\bullet\bullet}} - t_{e'} d\mu_{e'} \right) \quad (2)$$

Here, we consider the following local equilibria everywhere in the electrolyte



Considering eqs. (3) to (5) are the reaction in homogeneous phase, the following differential type equations are obtained from the balance of electrochemical potentials.

*Passed away in 2008

$$\frac{1}{2}d\mu_{\text{H}_2} + d\mu_{\text{h}} = d\mu_{\text{H}_i} \quad (6)$$

$$\frac{1}{2}d\mu_{\text{O}_2} + d\mu_{\text{V}_o} = 2d\mu_{\text{h}} \quad (7)$$

$$d\mu_{e'} + d\mu_{\text{h}} = 0 \quad (8)$$

where, as the concentration of normal oxide ion does not change so largely, it is estimated that $\mu_{\text{O}_o} = \text{const}$.

Furthermore, using the relationship of $t_{\text{H}_i} + t_{\text{h}} + t_{\text{V}_o} + t_{e'} = 1$ and substituting eqs. (6) to (8) into eq. (2), we get the following equation.

$$d\varphi = -\frac{1}{F} \left(d\mu_{\text{H}_i} - \frac{1}{2}d\mu_{\text{H}_2} + \frac{1}{2}t_{\text{H}_i}d\mu_{\text{H}_2} - \frac{1}{4}t_{\text{V}_o}d\mu_{\text{O}_2} \right) \quad (9)$$

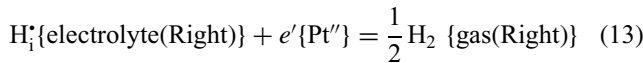
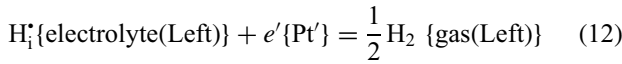
Integrating the both sides of the above equation from the left to the right end of the electrolyte, we get,

$$\int_{\varphi'}^{\varphi''} d\varphi = -\frac{1}{F} \int_{\mu_{\text{H}_i}'}^{\mu_{\text{H}_i}''} d\mu_{\text{H}_i} + \frac{1}{2F} \int_{\mu_{\text{H}_2}'}^{\mu_{\text{H}_2}''} d\mu_{\text{H}_2} - \frac{1}{2F} \int_{\mu_{\text{H}_2}'}^{\mu_{\text{H}_2}''} t_{\text{H}_i}d\mu_{\text{H}_2} + \frac{1}{4F} \int_{\mu_{\text{O}_2}'}^{\mu_{\text{O}_2}''} t_{\text{V}_o}d\mu_{\text{O}_2} \quad (10)$$

Thus, the potential difference between the ends of the electrolyte could be represented as follows.

$$\varphi'' - \varphi' = -\frac{1}{F}(\mu_{\text{H}_i}'' - \mu_{\text{H}_i}') + \frac{1}{2F}(\mu_{\text{H}_2}'' - \mu_{\text{H}_2}') - \frac{1}{2F} \int_{\mu_{\text{H}_2}'}^{\mu_{\text{H}_2}''} t_{\text{H}_i}d\mu_{\text{H}_2} + \frac{1}{4F} \int_{\mu_{\text{O}_2}'}^{\mu_{\text{O}_2}''} t_{\text{V}_o}d\mu_{\text{O}_2} \quad (11)$$

In the meantime, the following heterogeneous equilibria are being established among the electrolyte, platinum electrode and surrounding atmosphere.



Therefore, taking the balance of the electrochemical potentials of both sides of eqs. (12) and (13),

$$(\mu_{\text{H}_i}' + F\varphi') + (\mu_{e'} - F\varphi_{\text{Pt}'}) = \frac{1}{2}\mu_{\text{H}_2}' \quad (14)$$

$$(\mu_{\text{H}_i}'' + F\varphi'') + (\mu_{e''} - F\varphi_{\text{Pt}'}) = \frac{1}{2}\mu_{\text{H}_2}'' \quad (15)$$

where $\mu_{e'}$, $\mu_{e''}$ are the chemical potentials of the electrons in each platinum electrode at the same temperature, therefore, $\mu_{e'} = \mu_{e''}$.

Subtracting eq. (15) from eq. (14) side by side, we get

$$\varphi'' - \varphi' = -\frac{1}{F}(\mu_{\text{H}_i}'' - \mu_{\text{H}_i}') + \frac{1}{2F}(\mu_{\text{H}_2}'' - \mu_{\text{H}_2}') + (\varphi_{\text{Pt}''} - \varphi_{\text{Pt}'}) \quad (16)$$

By substituting eq. (16) into eq. (11), we get the emf of the cell $E = \varphi_{\text{Pt}''} - \varphi_{\text{Pt}'}$ as follows,

$$E = -\frac{1}{2F} \int_{\mu_{\text{H}_2}'}^{\mu_{\text{H}_2}''} t_{\text{H}_i}d\mu_{\text{H}_2} + \frac{1}{4F} \int_{\mu_{\text{O}_2}'}^{\mu_{\text{O}_2}''} t_{\text{V}_o}d\mu_{\text{O}_2} \quad (17)$$

Based on this equation, the emf is considered as the sum of the term of hydrogen potential difference and the term of oxygen potential difference.

Here, we examine the emf of this cell in the following specific conditions of the electrode potentials.

$$(1) \mu_{\text{O}_2}' = \mu_{\text{O}_2}''$$

In this case, the latter term of eq. (17) can be neglected. The emf of this hydrogen concentration cell is shown as follows using the activity of hydrogen p_{H_2} .¹²⁾

$$E = \frac{1}{4F} \int_{\mu_{\text{H}_2}'}^{\mu_{\text{H}_2}''} t_{\text{H}_i}d\mu_{\text{H}_2} = \frac{RT}{4F} \int_{\ln p_{\text{H}_2}'}^{\ln p_{\text{H}_2}''} t_{\text{H}_i}d \ln p_{\text{H}_2} \quad (18)$$

$$(2) \mu_{\text{H}_2}' = \mu_{\text{H}_2}''$$

In this case, the former term of eq. (17) can be neglected. The emf of this oxygen concentration cell is shown as follows.

$$E = \frac{1}{4F} \int_{\mu_{\text{O}_2}'}^{\mu_{\text{O}_2}''} t_{\text{V}_o}d\mu_{\text{O}_2} = \frac{RT}{4F} \int_{\ln p_{\text{O}_2}'}^{\ln p_{\text{O}_2}''} t_{\text{V}_o}d \ln p_{\text{O}_2} \quad (19)$$

$$(3) \mu_{\text{H}_2\text{O}}' = \mu_{\text{H}_2\text{O}}''$$

In this condition, we can assume $\mu_{\text{H}_2\text{O}} = \text{const}$ throughout the electrolyte. Therefore, using the equilibrium relation $\text{H}_2 + \frac{1}{2}\text{O}_2 = \text{H}_2\text{O}$, we get,

$$-2d\mu_{\text{H}_2} = d\mu_{\text{O}_2} \quad (20)$$

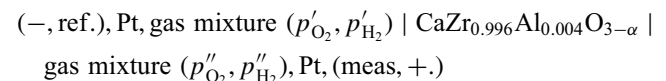
Thus, the emf is represented using eq. (17) as follows,

$$\begin{aligned} E &= -\frac{1}{2F} \int_{\mu_{\text{H}_2}'}^{\mu_{\text{H}_2}''} (t_{\text{H}_i} + t_{\text{V}_o})d\mu_{\text{H}_2} \\ &= \frac{1}{4F} \int_{\mu_{\text{O}_2}'}^{\mu_{\text{O}_2}''} (t_{\text{H}_i} + t_{\text{V}_o})d\mu_{\text{O}_2} \\ &= -\frac{RT}{2F} \int_{\ln p_{\text{H}_2}'}^{\ln p_{\text{H}_2}''} (t_{\text{H}_i} + t_{\text{V}_o})d \ln p_{\text{H}_2} \\ &= \frac{RT}{4F} \int_{\ln p_{\text{O}_2}'}^{\ln p_{\text{O}_2}''} (t_{\text{H}_i} + t_{\text{V}_o})d \ln p_{\text{O}_2} \end{aligned} \quad (21)$$

In this paper, this cell is called the hydrogen-oxygen concentration cell.

2.2 Cell assembly

The electrolyte used in this study was a sintered polycrystalline tube of the composition $\text{CaZr}_{0.996}\text{Al}_{0.004}\text{O}_{3-\alpha}$ supplied from TYK Corporation. The tube was closed at one end and 15 mm outer diameter, 12 mm inner diameter and 330 mm length. Porous platinum electrodes were applied to both the inner and outer surfaces over 10 mm from the tip of the closed end of the tube. The porous platinum coating was prepared by painting with commercial platinum paste and firing in the air. Platinum lead wire was attached to the electrode by sintering. The following gas concentration cell was composed using the outer and the inner electrode as the standard and the measuring one, respectively.



The oxygen and hydrogen activity at the electrode were controlled by the gas mixture $\text{H}_2\text{O}-\text{H}_2-\text{Ar}$ supplied to the electrode and equilibrated at the measurement temperature. The mixing ratio was controlled by ensuring that the mixture of H_2/Ar of predetermined ratio were over-saturated with water vapor and then equilibrated in a heat bath held at a constant temperature to adjust the water vapor to the desired

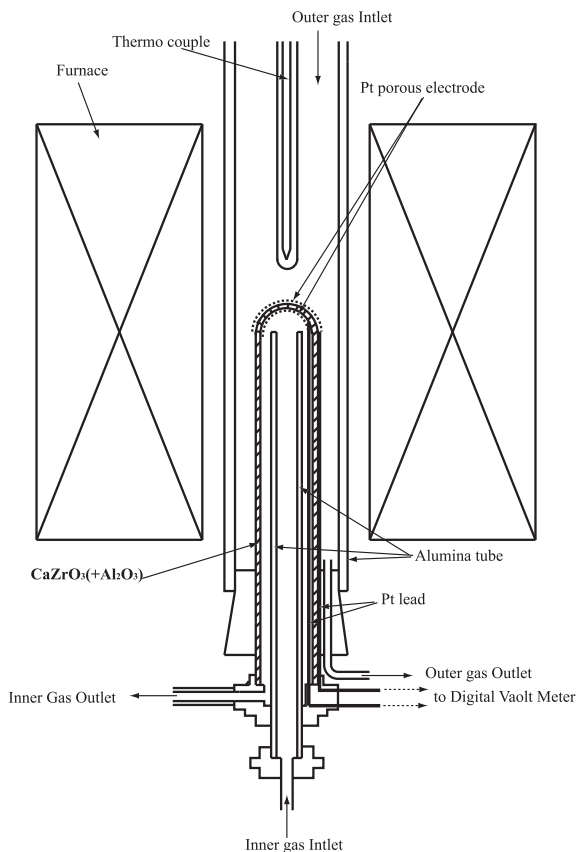


Fig. 1 Schematic view of experimental apparatus.

partial pressure. For a more detailed procedure of the activities control, another paper¹³⁾ should be consulted.

The schematic view of the cell assembly was shown in Fig. 1. The emf measurement was performed at temperatures from 973 to 1473 K with an interval of 100 K.

3. Results

3.1 Response of the emf

Figure 2 shows the emf change at 1373 K when the hydrogen activity of the measuring electrode was changed by keeping the activities of the reference electrode at $p'_{\text{H}_2\text{O}} = 0.01$, $p'_{\text{H}_2} = 0.01$. In this measurement, the water vapor concentration in the gas mixture supplied to the measuring electrode was changed simultaneously so as to keep the oxygen activity at both electrodes at the same value of 3.82×10^{-14} . As shown in the picture, the emf changes prominently by the change of partial pressure of hydrogen. Considering the capacity of the experimental apparatus and the gas flow rate (100 cc/min), the time needed for change is nearly the same as that required for the gas substitution in the equipment. Therefore, the emf seems to follow the change of gas activity immediately. Approximately 2 mV of emf was measured under the condition that the activities of hydrogen and oxygen on both electrodes were completely the same with each other. It was assumed that it occurred from the thermal electromotive force due to the inevitable small temperature difference between the outer and the inner side of the electrolyte. Therefore, regarding these emf's as the background of the measured value, all the reported emf values were corrected for it.

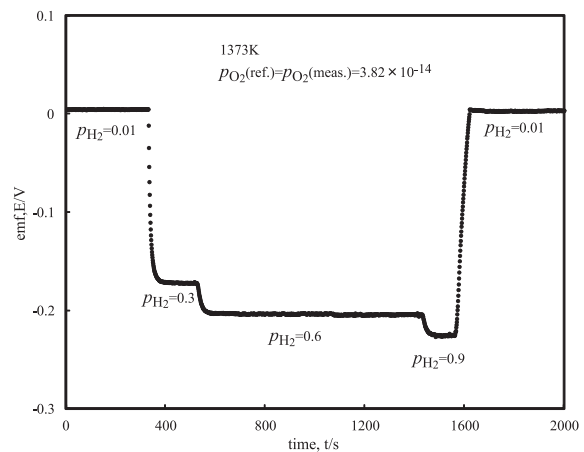


Fig. 2 Emf responses to the changes of gas compositions.

3.2 The emf of hydrogen concentration cell

Figure 3 shows the emf of the hydrogen concentration cell plotted against the hydrogen activity of the measuring electrode at the temperatures 973, 1073, 1173, 1273, 1373 and 1473 K. In each measurement, the oxygen activities of both electrodes were kept at the same constant value, which is shown in each figure. The solid line in the pictures represents the following Nernst equation, which is valid when the transport number of proton is unity.

$$E = -\frac{RT}{2F} \ln \frac{P'_{\text{H}_2}}{P'_{\text{H}_2}} \quad (22)$$

where E is the emf, R is the gas constant, T is the absolute temperature, and F is the faraday constant. The measured value coincides well with this calculated value. Therefore, in a hydrogen-rich atmosphere, the transport number of proton is unity over the wide temperature range investigated.

3.3 The emf of oxygen concentration cell

Figure 4 shows the emf of the oxygen concentration cell plotted against the oxygen activity of the measuring electrode. In each measurement, the hydrogen activities of both electrodes were kept at the same constant value, which is shown in each figure. The solid lines in the pictures represent the following Nernst equation, which is valid when the transport number of oxide ion vacancy is unity.

$$E = \frac{RT}{4F} \ln \frac{P'_{\text{O}_2}}{P'_{\text{O}_2}} \quad (23)$$

Under such a hydrogen-rich atmosphere any oxygen potential gradient does not generate significant emf and it was concluded that the transport number of oxygen ion vacancy at hydrogen-rich atmosphere is almost negligible.

3.4 The emf of hydrogen-oxygen concentration cell

Figure 5 shows the emf of the hydrogen-oxygen concentration cell plotted against the hydrogen activity of the measuring electrode. In each measurement, the water vapor activities of both electrodes were kept at the same constant value, which is shown in each figure. The solid lines in the pictures represent the following theoretical emf, which was derived from eq. (21) with the assumption that the sum of the transport number of proton and oxide ion is unity.

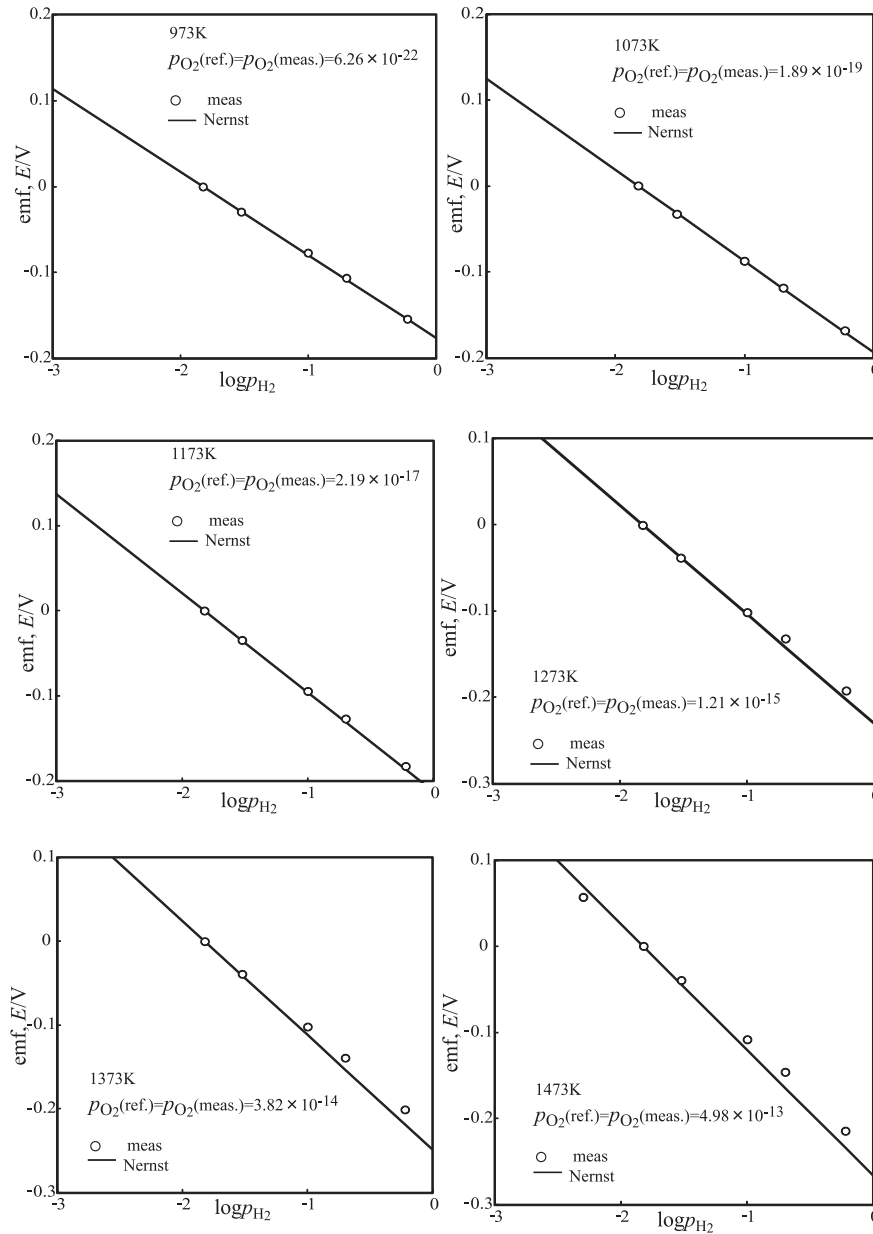


Fig. 3 Electromotive force of hydrogen concentration cell.

$$E = -\frac{RT}{2F} \ln \frac{P''_{\text{H}_2}}{P'_{\text{H}_2}} = \frac{RT}{4F} \ln \frac{P''_{\text{O}_2}}{P'_{\text{O}_2}} \quad (24)$$

Measured values were in good agreement with estimated ones in wide temperature and surrounding water vapor activity ranges. As has been already mentioned in section 3.1 and 3.2, the transport number of proton is almost unity and that of oxygen ion vacancy can be ignored, therefore, the obtained results were reasonable.

4. Discussion

4.1 The theoretical evaluation of emf using conduction parameter

In the previous work, we reported the conduction parameters derived based on the model of a defect structure and the data of the electrical conductivity measurements. Now, we estimate the theoretical emf's using these

parameters and compare them with the measured ones in order to confirm the validity of the conduction parameters.

As the transport number of proton was found to be dominant in almost all regions of temperatures and atmospheres investigated, these examinations were conducted only for cells operated at the highest temperature 1473 K where the effect of other charge carriers became significant.

Here, we consider the model of defect structure identical to that used in the previous report.¹⁰⁾ Namely, the movable defects are the interstitial proton, the oxide ion vacancy and the positive hole and they are in local equilibrium represented by eqs. (3) and (4). Moreover, the concentration of positive hole is far less than those of the proton and the oxide ion vacancy. In that situation, the electrical neutrality condition is represented using the 'active' dopant concentration $[Al'_{\text{Zr}}]$ as follows.

$$[H_i^+] + 2[V_O^{\bullet\bullet}] = [Al'_{\text{Zr}}] \quad (25)$$

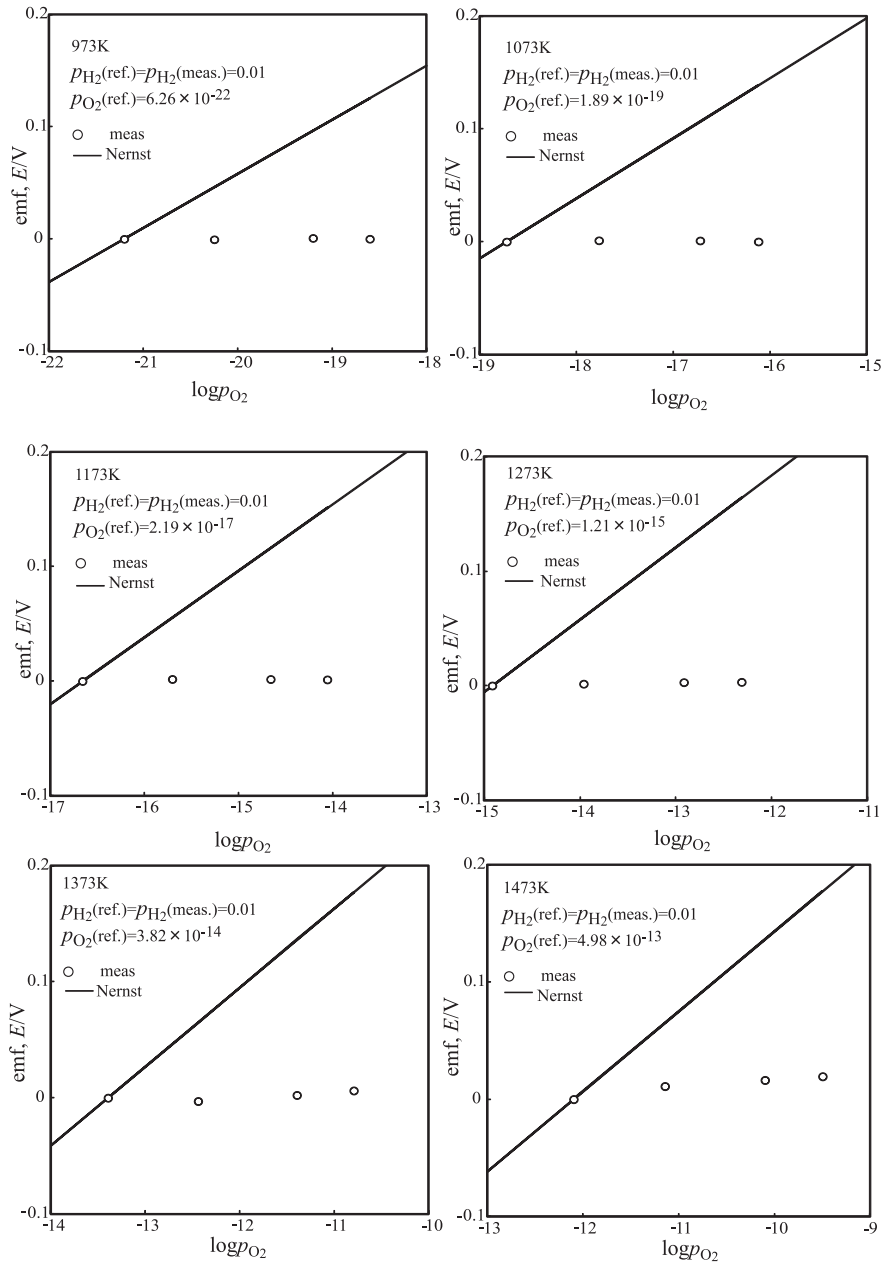


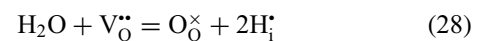
Fig. 4 Electromotive force of oxygen concentration cell.

In this case, the concentration of the proton and the oxide ion vacancy are given as a function of the activity of water vapor as follows,¹⁰⁾

$$[H_i^+] = \frac{-\frac{K_5 P_{H_2O}}{2} + \sqrt{\left(\frac{K_5 P_{H_2O}}{2}\right)^2 + 2K_5 P_{H_2O}[Al'_{Zr}]}}{2} \quad (26)$$

$$[V_o^{\bullet\bullet}] = \frac{[Al'_{Zr}]}{2} - \frac{-\frac{K_5 P_{H_2O}}{2} + \sqrt{\left(\frac{K_5 P_{H_2O}}{2}\right)^2 + 2K_5 P_{H_2O}[Al'_{Zr}]}}{4} \quad (27)$$

where K_5 is the equilibrium constant of the apparent equation of the hydrogen dissolution represented as follows.



The value of K_5 was determined in the previous report¹⁰⁾ as follows,

$$\Delta G^\circ / J \text{ mol}^{-1} = -RT \ln(K_5) = 170,000 + 160T \quad (29)$$

Therefore, the concentration of proton and oxide ion vacancy can be calculated depending on the individual activity of the surrounding atmosphere when the concentration of the active dopant $[Al'_{Zr}]$ is known.

Furthermore, in the previous report, the mobility $m_{H_i^+}$ of the interstitial proton, and the mobility $m_{V_o^{\bullet\bullet}}$ of oxygen ion vacancy were estimated as follows.¹⁰⁾

$$m_{H_i^+} / \text{cm}^2 \text{ s}^{-1} \text{ V}^{-1} = \frac{0.137}{T} \exp\left\{-\frac{0.85 \text{ eV}}{kT}\right\} \quad (30)$$

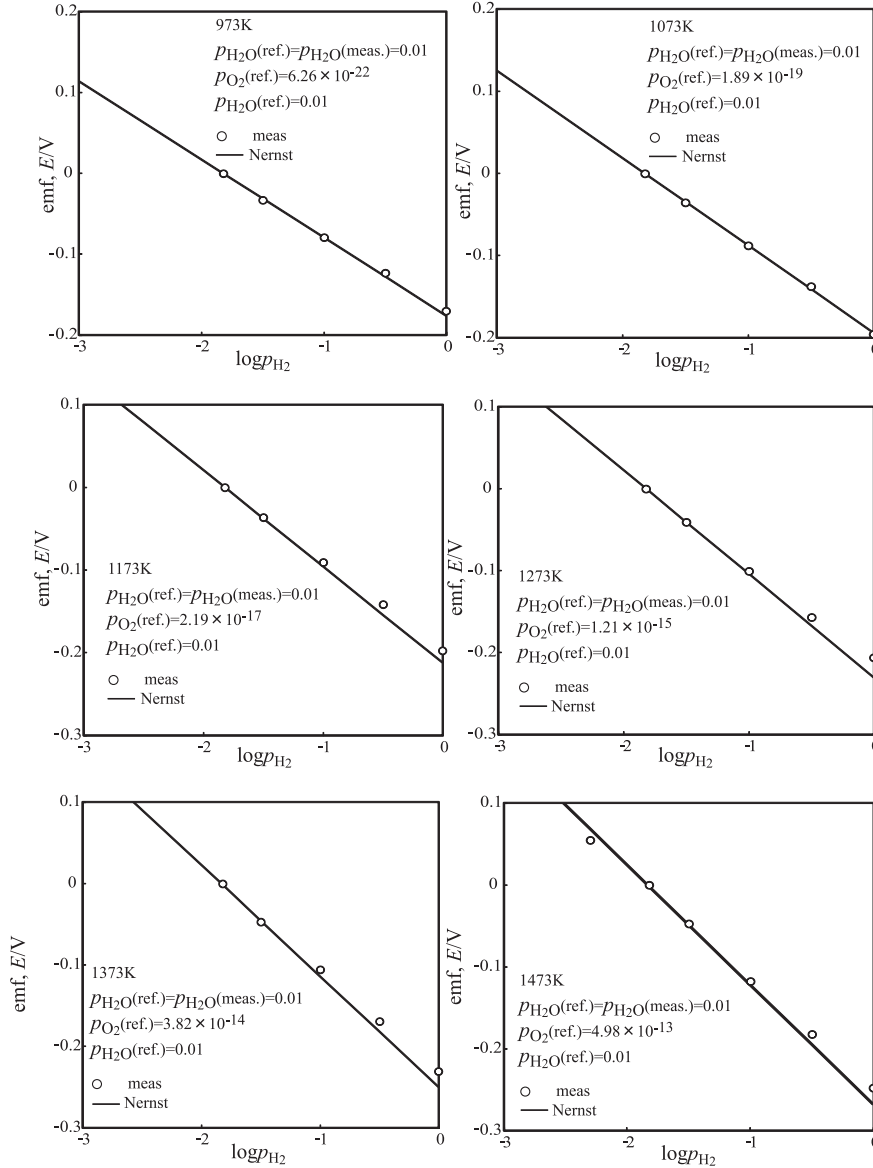


Fig. 5 Electromotive force of hydrogen-oxygen concentration cell.

$$m_{V_o^{\bullet}}/\text{cm}^2 \text{ s}^{-1} \text{ V}^{-1} = \frac{0.0004}{T} \exp\left\{-\frac{2.3 \text{ eV}}{kT}\right\} \quad (31)$$

$$t_{V_o^{\bullet}} = \frac{\sigma_{V_o^{\bullet}}}{\sigma_{H_i^{\bullet}} + \sigma_{V_o^{\bullet}}} \quad (34)$$

Based on these values, the partial electrical conductivity of the interstitial proton and oxygen ion vacancy could be evaluated as a function of water vapor activity.

When equilibrium between the electrolyte and electrode is attained, the transport number of each charge carrier can be generally represented by the conductivities as follows:

$$t_i = \frac{\sigma_i}{\sum_i \sigma_i} \quad (32)$$

Therefore, in the situation of hydrogen-rich atmosphere where the conduction of positive hole may be ignored, the transport number of interstitial proton $t_{H_i^{\bullet}}$, and oxygen ion vacancy $t_{V_o^{\bullet}}$ are represented as follows:

$$t_{H_i^{\bullet}} = \frac{\sigma_{H_i^{\bullet}}}{\sigma_{H_i^{\bullet}} + \sigma_{V_o^{\bullet}}} \quad (33)$$

Using the eqs. (26), (27), (30), (31), (33), (34), each transport number can be obtained as a function of the activity of the water vapor.

Meanwhile, about the hydrogen concentration cell or the oxygen concentration cell, the value of activity of oxygen or hydrogen which was kept constant respectively at both electrodes is considered to be maintained even inside of the electrolyte. Activity of water vapor, therefore, can be fixed any point in the electrolyte and then transport number of proton or oxide ion can be calculated for the individual increments of the chemical potential of hydrogen or oxygen. Namely, the integration in eq. (18) or (19) can be calculated numerically from the above conduction parameters.

For the hydrogen-oxygen concentration cell, the integration is much easier because the term of the sum of the

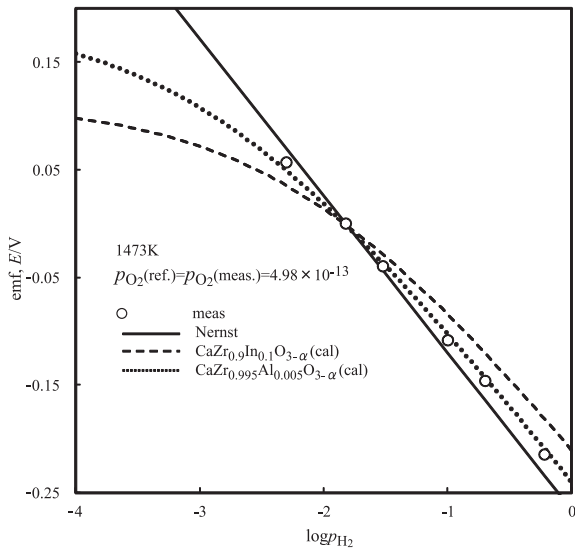


Fig. 6 Comparison of theoretical emf with measured value in hydrogen concentration cell operated at 1473 K.

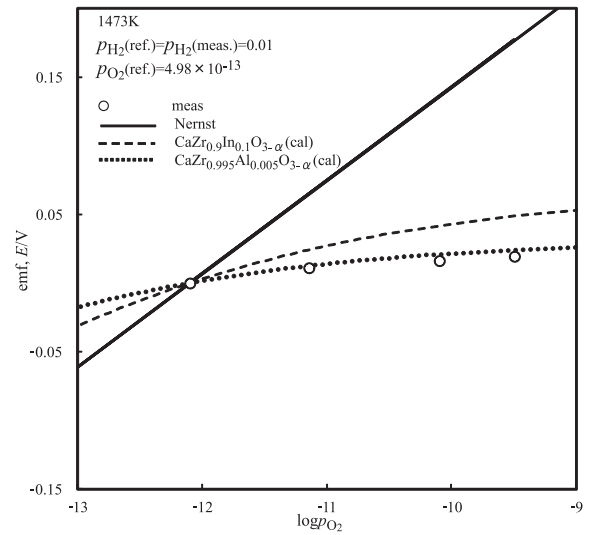


Fig. 7 Comparison of theoretical emf with measured value in oxygen concentration cell operated at 1473 K.

transport number of proton and oxide ion vacancy is fixed to the individual constant water vapor activity given to the cell. Therefore, the term can be left out of the integrand.

Although the concentration of dopant of the electrolyte is 0.4 mol% and a slightly less than that of the specimen for which the conduction parameters were determined (0.5 mol%), the same parameters were used in the calculation only modifying the amount of dopant active for the proton incorporation. Based on the considerations in the previous work, only 1/10 of the total amount of dopant was estimated to be active. Therefore, the value $[Al'_{Zr}] = 0.0004$ was used in the present calculation. This means that 90% of the dopant exists as the neutral associate defect, for example, $(Al_{Zr}V_O Al_{Zr})^\times$ and are not participating in the proton incorporation. This hypothesis must be verified further but looks reasonable at this moment.

Figures 6, 7, and 8 shows the comparison between the measured emf and the theoretical ones calculated with the above procedures for the hydrogen, the oxygen and the hydrogen-oxygen concentration cell, respectively. As shown in the figures, the calculated and the measured emf's showed coincidence with each other for all measurements. Therefore, it was confirmed that the conduction parameters determined from the conductivity measurement of $CaZr_{0.995}Al_{0.005}O_{3-\alpha}$ were reasonable.

In Figs. 6 and 7, the estimated emf's for the cell employing $CaZr_{0.9}In_{0.1}O_{3-\alpha}$ as the electrolyte were also contained. They were calculated using the following equations and conduction parameters that had been reported elsewhere.¹³⁾

$$E = -\frac{RT}{F} \ln \frac{p''_{H_2}{}^{1/2} + w_1}{p'_{H_2}{}^{1/2} + w_1} - \frac{RT}{F} \ln \frac{p''_{O_2}{}^{-1/4} + w_2}{p'_{O_2}{}^{-1/4} + w_2}$$

where

$$w_1 = \frac{\sigma_{V_O}^{\circ} + \sigma_{H_i}^{\circ} p''_{O_2}{}^{1/4}}{\sigma_{H_i}^{\circ} K^{-1/2} p''_{O_2}{}^{1/4}}, w_2 = \frac{\sigma_{H_i}^{\circ} K^{-1/2} p'_{H_2}{}^{1/2} + \sigma_{H_i}^{\circ}}{\sigma_{V_O}^{\circ}}$$

and

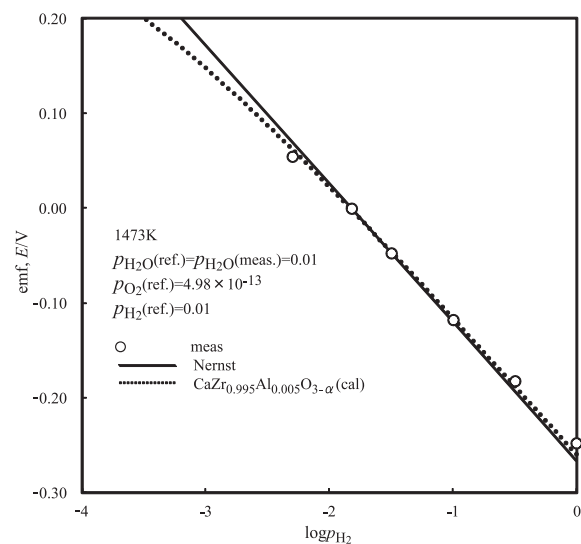


Fig. 8 Comparison of theoretical emf with measured value in hydrogen-oxygen concentration cell operated at 1473 K.

$$\sigma_{H_i}^{\circ} = \frac{10^{4.25}}{T} \exp\left(-\frac{0.775}{kT}\right)$$

$$\sigma_{V_O}^{\circ} = \frac{10^{8.89}}{T} \exp\left(-\frac{2.47}{kT}\right)$$

$$\sigma_{H_i}^{\circ} = \frac{10^{5.22}}{T} \exp\left(-\frac{1.18}{kT}\right)$$

In the hydrogen concentration cell, the obtained emf (the absolute value of the emf) of the cell based on $CaZr_{0.996}Al_{0.004}O_{3-\alpha}$ is larger than that of the cell based on $CaZr_{0.9}In_{0.1}O_{3-\alpha}$. This implies that the transport number of proton is larger in $CaZr_{0.996}Al_{0.004}O_{3-\alpha}$ than in $CaZr_{0.9}In_{0.1}O_{3-\alpha}$ in this region of atmosphere. On the contrary, for the oxygen concentration cell, the obtained emf of the cell based on $CaZr_{0.996}Al_{0.004}O_{3-\alpha}$ is smaller than that based on

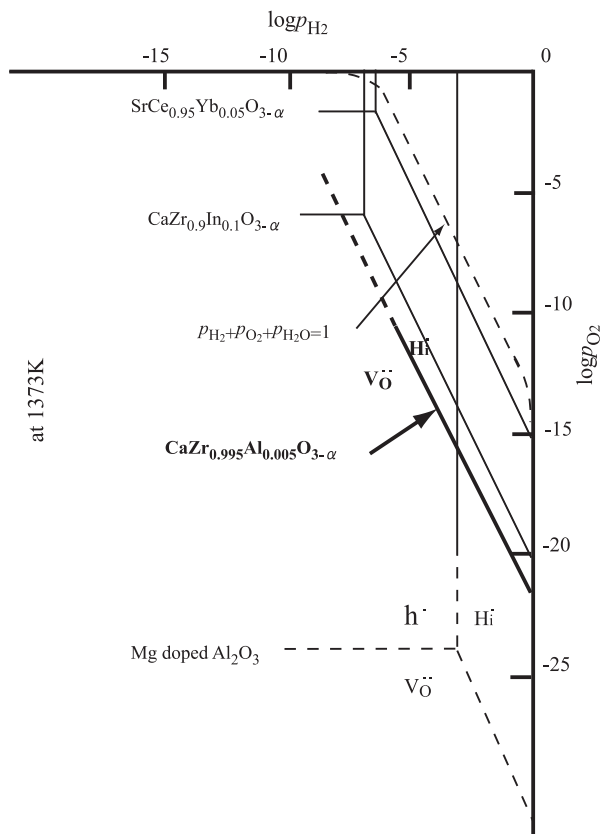


Fig. 9 Comparison of the conduction domain diagrams at 1373 K.

CaZr_{0.9}In_{0.1}O_{3- α} . This suggests that the degeneration of the conduction of proton in CaZr_{0.996}Al_{0.004}O_{3- α} with the growth of the conduction of oxide ion commences at lower oxygen activity than in CaZr_{0.9}In_{0.1}O_{3- α} .

4.2 Conduction domain diagram

By using the conduction parameters determined above, the transport number of proton and oxide ion vacancy can be estimated at any temperature and atmosphere conditions. Therefore, we can evaluate the values of the hydrogen and the oxygen activity at which the both transport numbers are identical and can determine a part of the boundary of the conduction domain diagram. In Fig. 9, the boundary between the conduction domain of the proton and that of the oxide ion vacancy thus determined. In the figure, the domain diagrams reported for other systems¹⁴⁾ were also contained. Although the boundary against the conduction domain of the positive holes have not been cleared yet, the conduction domain of proton for Al-doped CaZrO₃ seems to be a little wider than that for In-doped CaZrO₃.

5. Conclusion

The following gas concentration cell using CaZr_{0.996}Al_{0.004}O_{3- α} as the electrolyte was made and its emf's were measured for various setups of the activity gradient.

(-, ref.), Pt, gas mixture ($p'_{\text{O}_2}, p'_{\text{H}_2}$) | CaZr_{0.996}Al_{0.004}O_{3- α} | gas mixture ($p''_{\text{O}_2}, p''_{\text{H}_2}$), Pt, (meas, +.)

Under the hydrogen-rich atmosphere investigated, it was found that the emf generated only with the hydrogen activity gradient. The detailed analysis of the obtained emf data showed that the transport number of proton in CaZr_{0.996}Al_{0.004}O_{3- α} is almost unity for the hydrogen-rich atmosphere and its proton conduction domain is a little wider than that of the In doped CaZrO₃ system.

The measured emf's obtained for the condition where the transport number of the proton was less than unity were in good agreement with the theoretical ones calculated using the conduction parameters determined by the previous work on the conductivity measurements. The conduction parameter, and therefore, the model of the defect structure presented in the previous paper for CaZr_{0.995}Al_{0.005}O_{3- α} were confirmed reasonable.

Acknowledgements

We dedicate this paper to the memory of Mr. Hiroyuki Ohno, one of the authors, who had made an important contribution to this work in the early stage of the research and passed away due to a traffic accident before the publication of this paper.

This work was supported in part by a grant from the Institute of Ceramics Research and Education at NITECH, a Grant-in Aid Science Research (19206081) from the Ministry of Education, Culture, Sports, Science and Technology in Japan, and a grant of SENTAN from JST.

REFERENCES

- 1) T. Yajima, K. Koide, N. Fukatsu, T. Ohashi and H. Iwahara: *Keikinzoku* **42** (1992) 263.
- 2) T. Yajima, K. Koide, N. Fukatsu, T. Ohashi and H. Iwahara: *Sens. Actuators B Chem.* **14** (1993) 697–699.
- 3) H. Iwahara, T. Shimura and H. Matsumoto: *Electrochem.* **68** (2000) 154.
- 4) N. Kurita, N. Fukatsu, S. Miyamoto, F. Sato, H. Nakai, K. Irie and T. Ohashi: *Metall. Mater. Trans. B* **12** (1996) 27B.
- 5) N. Kurita, N. Fukatsu, A. Naito, K. Koide and T. Ohashi: *Shigen to Sozai* **113** (1997) 45.
- 6) H. Iwahara: *Solid State Ion.* **52** (1992) 99.
- 7) J. R. Frade: *Solid State Ion.* **78** (1995) 87.
- 8) H. K. Benter, N. Bonaons and J. W. Phair: *Solid State Ion.* **181** (2010) 249.
- 9) Y. C. Yang, J. Park, J. Kim, Y. Kim and J. O. Park: *Ionics* **16** (2010) 397.
- 10) J. Bao, H. Ohno, N. Kurita, Y. Okuyama and N. Fukatsu: *Electrochim. Acta* **56** (2010) 1062.
- 11) C. Wagner: *Z. Physical. Chem. B* **21** (1933) 25.
- 12) All p 's in this paper represent activities of the denoted gas species whose standard state is taken as the respective pure gas at the pressure of 1 bar.
- 13) N. Kurita, K. Ootake and N. Fukatsu: *J. Electrochem. Soc.* **158** (2011) B667.
- 14) N. Fukatsu and N. Kurita: *Proc. Masuko Symposium, The 16th Iketani Conference, vol. 16, (2006) pp. 361–394.*